Detecting Out-of-Time-Order Correlations via Quasiadiabatic Echoes as a Tool to Reveal Quantum Coherence in Equilibrium Quantum Phase Transitions

R. J. Lewis-Swan,[1,2,3] S. R. Muleady,[2,3] and A. M. Rey[2,3]
[1]Homer L. Dodge Department of Physics and Astronomy, The University of Oklahoma, Norman, Oklahoma 73019, USA
[2]JILA, NIST, Department of Physics, University of Colorado, Boulder, Colorado 80309, USA
[3]Center for Theory of Quantum Matter, University of Colorado, Boulder, Colorado 80309, USA

(Received 11 June 2020; revised 9 September 2020; accepted 26 October 2020; published 10 December 2020)

We propose a new dynamical method to connect equilibrium quantum phase transitions and quantum coherence using out-of-time-order correlations (OTOCs). Adopting the iconic Lipkin-Meshkov-Glick and transverse-field Ising models as illustrative examples, we show that an abrupt change in coherence and entanglement of the ground state across a quantum phase transition is observable in the spectrum of multiple quantum coherence intensities, which are a special type of OTOC. We also develop a robust protocol to obtain the relevant OTOCs using quasi-adiabatic quenches through the ground state phase diagram. Our scheme allows for the detection of OTOCs without time reversal of coherent dynamics, making it applicable and important for a broad range of current experiments where time reversal cannot be achieved by inverting the sign of the underlying Hamiltonian.

DOI: 10.1103/PhysRevLett.125.240605

Introduction.—Quantum phase transitions (QPTs) [1] play a central role in many fields of quantum science and have been studied using a variety of tools. Fundamentally, a QPT is signaled in the thermodynamic limit by a nonanalyticity in the energy density of the ground state or a vanishing energy gap between the ground and lowest-excited states. However, quantum information science has ignited a theoretical push toward characterizing the critical region of a QPT through information-theoretic quantities such as entanglement entropy [2–4], Loschmidt echoes [5,6], fidelity susceptibility [7–9], and coherence measures [10–14].

In parallel, the past two decades have seen a growing focus on the dynamics of quantum information [15] and nonequilibrium systems [16] as a result of improvements in the technical capabilities of atomic, molecular, and optical (AMO) experiments. Of recent note is the study of quantum chaos and information scrambling using out-of-time-order correlations (OTOCs) [17–20]. Already, OTOCs have been adapted to study phenomena beyond their original purview, including the diagnosis of dynamical [21,22] and equilibrium phase transitions [23–25]. Recent work has also demonstrated that a special type of fidelity OTOC (FOTOC) [26] can be a powerful tool to diagnose entanglement [27] and coherence [28] in many-body systems through the framework of multiple quantum coherences (MQCs) pioneered in NMR [29–31].

Motivated by these developments, here, we demonstrate that FOTOCs and the spectrum of MQC intensities can serve as a unifying tool to connect concepts of quantum coherence to equilibrium QPTs in a dynamical setting. In doing so, we also develop a powerful new protocol to dynamically access FOTOCs, distinct from recent schemes in that we do not require time reversal via altering the sign of the Hamiltonian [26,28,32–35], nor do we demand auxiliary qubits [36–38] or exhaustive measurements [39–41].

In this Letter, we utilize the paradigmatic Lipkin-Meshkov-Glick (LMG) and transverse-field Ising (TFI) models as case studies to demonstrate that FOTOCs can diagnose the nonanalyticity of a QPT and can distinguish quantum phases even in the limit of small system size. We illustrate the power of FOTOCs as a practical tool for the characterization of QPTs by proposing a completely general, experimentally realistic dynamical protocol to obtain these correlations and the related MQC spectrum from a pseudoecho of quasi-adiabatic dynamics. The technical simplicity of our scheme relative to the aforementioned alternatives means that our results are relevant for a broad range of experimentally accessible models in AMO and condensed matter physics in addition to the spin models studied here, with immediate impact for state-of-the-art quantum simulators. For example, relaxation of the time-reversal constraint opens the possibility to more easily study OTOCs in short-range Ising models simulated with trapped ions, similar to the TFI model we investigate.

Quantifying quantum coherence.—The FOTOCs we study are defined as $F_\phi = \mathrm{Tr}[\hat{W}_\phi^\dagger(t)\hat{\rho}_0\hat{W}_\phi(t)\hat{\rho}_0]$, where $\hat{W}(t) = \hat{U}^\dagger(t)e^{-i\phi\hat{A}}\hat{U}(t)$, $\hat{A}$ is a Hermitian operator, and $\hat{U}(t)$ describes a unitary time-evolution operator that will be specified later in the Letter. We connect FOTOCs to MQCs [26,27] using cyclicity of the trace to rewrite $F_\phi = \mathrm{Tr}[\hat{\rho}\hat{\rho}^\phi]$, where we define $\hat{\rho} = \hat{U}(t)\hat{\rho}_0\hat{U}^\dagger(t)$ and $\hat{\rho}^\phi \equiv e^{-i\phi\hat{A}}\hat{\rho}e^{i\phi\hat{A}}$. We have dropped the explicit time

dependence on $\hat{\rho}$ to simplify notation. The Fourier transform of the FOTOC F_ϕ then defines the spectrum of MQC intensities:

$$I_m^{\hat{A}}(\hat{\rho}) = \sum_\phi F_\phi e^{im\phi}.$$

The MQC intensities are a well-established signature of the coherence of a many-body state [29–31,42]. This can be seen using the alternative definition [27] $I_m^{\hat{A}}(\hat{\rho}) \equiv \mathrm{Tr}[\hat{\rho}_{-m}\hat{\rho}_m]$, where

$$\hat{\rho}_m = \sum_{\lambda_i - \lambda_j = m} \rho_{ij} |\lambda_i\rangle\langle\lambda_j|$$

with $|\lambda_i\rangle$ as the eigenstates of a given Hermitian operator $\hat{A}$ such that $\hat{A}|\lambda_i\rangle = \lambda_i|\lambda_i\rangle$. By construction, the blocks $\hat{\rho}_m$ contain all coherences between eigenstates of $\hat{A}$ differing by m, which is then quantified via $I_m^{\hat{A}}(\hat{\rho})$.

Signals of a QPT in MQCs.—Here, we show that the spectrum of MQC intensities, accessible via FOTOCs, allows a robust and experimentally accessible characterization of QPTs in terms of quantum coherence [10]. Our central insight is that the drastic change in the coherence and entanglement of a many-body ground state across a QPT should lead to a correspondingly sharp change in the features of the MQC spectrum for an appropriately chosen $\hat{A}$.

To formalize this statement, we consider a general toy Hamiltonian: $\hat{H} = \hat{H}_1 + \lambda\hat{H}_2$, where $[\hat{H}_1, \hat{H}_2] \neq 0$ and $\lambda \geq 0$ is a dimensionless (tunable) parameter. We take $\hat{A} = \hat{H}_2$ and consider the ground state in the limiting cases $\lambda \to 0$ and $\lambda \to \infty$. In the latter case, the ground state $|\psi_{\mathrm{GS}}^{\lambda\to\infty}\rangle$ of $\hat{H}$ is the lowest-energy eigenstate of $\hat{H}_2$, and thus $\hat{\rho}_{\mathrm{GS}}^{\lambda\to\infty} = |\psi_{\mathrm{GS}}^{\lambda\to\infty}\rangle\langle\psi_{\mathrm{GS}}^{\lambda\to\infty}|$ is composed of a single diagonal entry in the eigenbasis defined by $\hat{A} = \hat{H}_2$. Trivially, the MQC spectrum will then be composed of a single peak, $I_m^{\hat{H}_2}(\hat{\rho}_{\mathrm{GS}}^{\lambda\to\infty}) = \delta_{m,0}$, due to the lack of coherences with respect to $\hat{H}_2$. Conversely, for $\lambda \to 0$, the ground state $|\psi_{\mathrm{GS}}^{\lambda\to 0}\rangle$ becomes an eigenstate of $\hat{H}_1$. As $[\hat{H}_1, \hat{H}_2] \neq 0$, this ground state cannot be a simultaneous eigenstate of $\hat{H}_2$: $|\psi_{\mathrm{GS}}^{\lambda\to 0}\rangle$ must be a coherent superposition of eigenstates of $\hat{H}_2$ such that the density matrix $\hat{\rho}_{\mathrm{GS}}^{\lambda\to 0} = |\psi_{\mathrm{GS}}^{\lambda\to 0}\rangle\langle\psi_{\mathrm{GS}}^{\lambda\to 0}|$ possesses off-diagonal coherences with respect to the $\hat{H}_2$ eigenbasis. Consequently, we expect a (relatively) broad MQC spectrum with nonzero $I_m^{\hat{H}_2}(\hat{\rho}_{\mathrm{GS}}^{\lambda\to 0})$ for $m \neq 0$.

Extending the spirit of this argument between these two limits, we expect for a model possessing a QPT at a critical point λ_c that the transition will generically be signaled by an abrupt change from a narrow to broad MQC spectrum. This expectation can also be supported by the fact that the spectral width

$$2\sigma_{\mathrm{MQC}}^2 = 2\sum_m m^2 I_m^{\hat{H}_2}(\hat{\rho}_{\mathrm{GS}})$$

is a lower bound for the quantum Fisher information (QFI) [27,42,43] of the state $\hat{\rho}_{\mathrm{GS}}$ with respect to $\hat{H}_2$ (saturated for pure states). Prior work has shown the QFI can provide signatures of a QPT [44], although this was typically computed with respect to a known order parameter rather than $\hat{H}_2$. We proceed to show that not only the width of this MQC spectrum but also, more importantly, individual intensities themselves can signal a QPT. An experimentally relevant quantity is $I_0^{\hat{H}_2}$, which features a divergent derivative $(d^2/d\lambda^2)I_0^{\hat{H}_2}$ at the QPT in the thermodynamic limit.

Demonstrative examples.—We illustrate and validate our arguments with a pair of iconic models of quantum magnetism: the anisotropic LMG [45,46] and the one-dimensional TFI [47–49] models. The former describes an ensemble of N mutually interacting spin-1/2 particles in a transverse field, while the latter involves only nearest-neighbor interactions. Each model can be described within the general Hamiltonian

$$\hat{H} = -\frac{1}{2\mathcal{C}}\sum_{i<j}\chi_{ij}\hat{\sigma}_i^z\hat{\sigma}_j^z - \frac{\Omega}{2}\sum_i \hat{\sigma}_i^x, \tag{1}$$

where $\hat{\sigma}_i^\alpha$ are Pauli operators for site i, and $\alpha = x, y, z$. The interaction between spins at sites i and j is characterized by χ_{ij}, and Ω is the transverse-field strength. We normalize the interaction by

$$\mathcal{C} = \frac{(\sum_{i,j}\chi_{ij})}{\chi N}$$

for the LMG model $\chi_{ij} = \chi$; while for the TFI model, $\chi_{ij} = \chi\delta_{i,j-1}$. We adopt $\hbar = 1$ throughout the Letter.

Each model features a second-order QPT between ferromagnetic and paramagnetic phases at a critical point $(\Omega/\chi)_c = 1$. The ground state physics can be described within the basis of fully symmetric spin states $|m_\alpha\rangle$ defined by $\hat{S}_\alpha|m_\alpha\rangle = m_\alpha|m_\alpha\rangle$, where

$$\hat{S}_\alpha \equiv \sum_j (\hat{\sigma}_j^\alpha/2),$$

and we suppress the quantum number $S = N/2$ for brevity. In the strong-field limit $\Omega/\chi \gg 1$, the paramagnetic ground state is characterized by the polarization of all spins identically along $\hat{x}$, $|\psi_{\mathrm{GS}}^P\rangle = |(N/2)_x\rangle$; while in the weak-field limit $\Omega/\chi \ll 1$, the ferromagnetic ground state is an entangled Greenberger-Horne-Zeilinger state, $|\psi_{\mathrm{GS}}^F\rangle = |(N/2)_z\rangle \pm |-(N/2)_z\rangle$. We work with the symmetric state, which is adiabatically connected to the paramagnetic ground state for finite N.

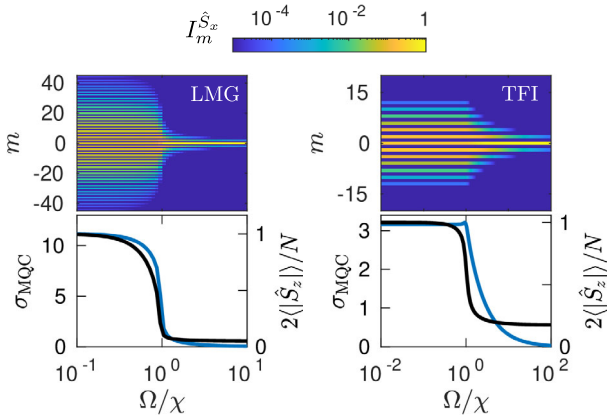

FIG. 1. Characteristic MQC spectra $I_m^{\hat{S}_x}(\hat{\rho}_{\mathrm{GS}})$ of the numerically computed ground state for the LMG ($N = 250$) and the analytically computed ground state for the TFI ($N = 20$) models as a function of Ω/χ. The phase boundary near $\Omega/\chi \approx 1$ in both models is signified by an abrupt change in the spectrum width σ_{MQC} (blue line, lower panels), which we also compare to the order parameter $\langle|\hat{S}_z|\rangle$ (black, lower panels).

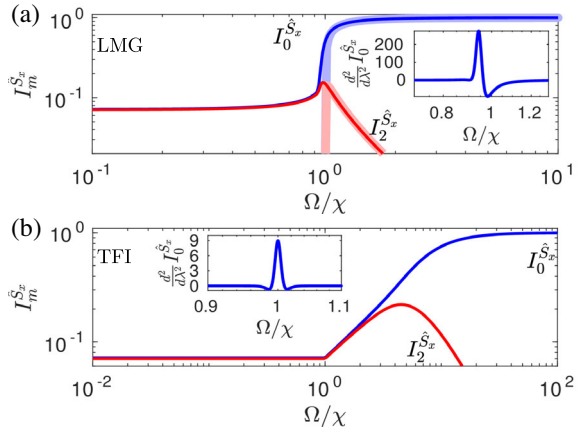

FIG. 2. Signatures of a QPT in the MQC intensities $I_m^{\hat{S}_x}$. (a) The LMG model in the $N \to \infty$ limit (faded lines) has abruptly vanishing intensities $I_0^{\hat{S}_x}$ (blue) and $I_2^{\hat{S}_x}$ (red) at the critical point, $(\Omega/\chi)_c = 1$. Dark lines indicate a numerical comparison for $N = 250$. (b) The TFI model displays a sharp kink in the $I_0^{\hat{S}_x}$ and $I_2^{\hat{S}_x}$ components at the critical point $(\Omega/\chi)_c = 1$. We plot results for the analytically computed ground state using $N = 250$ to facilitate comparison with the LMG results. Insets for Figs. 2(a) and 2(b) highlight the divergence in $d^2 I_0^{\hat{S}_x}/d\Omega^2$ at the QPT for $N = 250$.

Besides the growth of the width, we are also able to establish both analytically and numerically that the QPT is signaled directly in the individual MQC intensities (see Ref. [50] for relevant expressions). Our most relevant observation is that the derivative $d^2 I_0^{\hat{S}_x}(\hat{\rho}_{\mathrm{GS}})/d\Omega^2$ diverges at Ω_c as shown in Fig. 2. A similar feature is observable in $d^2 I_2^{\hat{S}_x}(\hat{\rho}_{\mathrm{GS}})/d\Omega^2$ [50].

For the LMG model, the location of the transition $(\Omega/\chi)_*$, taken as the peak of $d^2 I_0^{\hat{S}_x}(\hat{\rho}_{\mathrm{GS}})/d\Omega^2$ for a finite system, approaches the $N \to \infty$ critical point as $[1 - (\Omega/\chi)_*] \sim N^{-0.65}$ [50], consistent with that of $(\Omega/\chi)_*$ obtained from the peak in the susceptibility $(d/d\Omega)\langle|\hat{S}_z|\rangle$ over the same window of system size N. Similarly, for the TFI model, the location of the peak in $d^2 I_0^{\hat{S}_x}(\hat{\rho}_{\mathrm{GS}})/d\Omega^2$ approaches as $[1 - (\Omega/\chi)_*] \sim N^{-2}$ [50,62]. This verifies that the MQC signatures do not display any systematic offset from the QPT beyond finite size effects [63].

We also point out that the LMG model predicts a sharp peak in $I_{m>0}^{\hat{S}_x}(\hat{\rho}_{\mathrm{GS}})$ in the paramagnetic phase close to the QPT. This could serve as a more modest proxy for the QPT in experimental systems [50]. Conversely, the TFI model shows a similar peak, but it shifts further into the paramagnetic phase as N increases and is uncorrelated with the QPT.

The demonstration that the QPT is unambiguously signaled by an abrupt change of the spectral width and character of individual MQC intensities in both of these models, regardless of the fact that they belong to different universality classes, emphasizes the general utility of the MQC spectrum to diagnose a QPT.

Obtaining FOTOCs without time reversal.—The measurement of FOTOCs and the associated MQC spectrum has previously been achieved via echoes based on the time reversal of coherent dynamics [28,32]. This can be seen from the definition of the FOTOC given previously: $F_\phi = \mathrm{Tr}[\hat{W}_\phi^\dagger(t)\hat{\rho}_0\hat{W}_\phi(t)\hat{\rho}_0]$, where $\hat{W}_\phi(t) = \hat{U}^\dagger(t)e^{-i\phi\hat{A}}\hat{U}(t)$, which is interpreted as a dynamical sequence starting from the state $\hat{\rho}_0$ followed by (i) unitary evolution $\hat{U}(t)$, (ii) a perturbation $e^{-i\phi\hat{A}}$, (iii) time-reversed dynamics $\hat{U}^\dagger(t)$, and (iv) a projective measurement of the final overlap with $\hat{\rho}_0$. Here, we discuss an approach to obtain the MQC spectrum of a generic ground state $\hat{\rho}_{\mathrm{GS}}$ by a similar echo sequence that replaces the time-reversal step with adiabatic dynamics. This substitution opens the possibility of accessing OTOCs in a much broader range of physical platforms than previously considered.

The proposed echo sequence is shown in Fig. 3(a), where we concretely identify $\hat{U}(t)$ as describing a slow ramp of

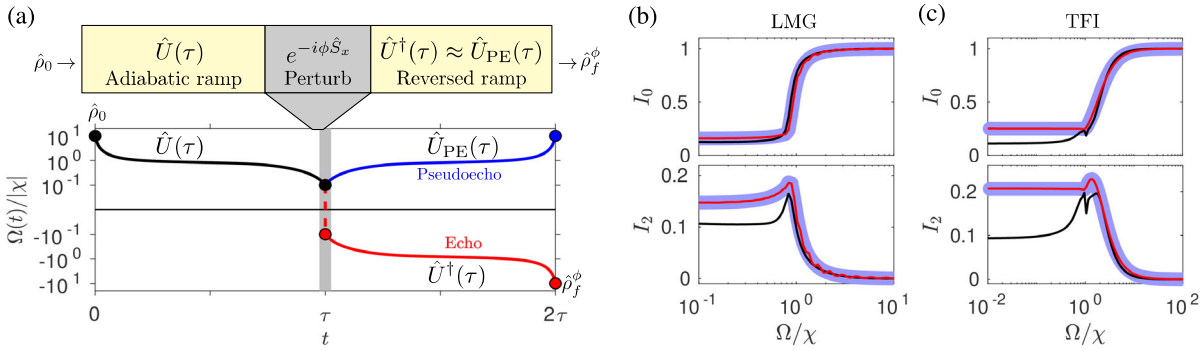

FIG. 3. (a) Schematic of many-body echo to obtain the MQC spectrum. The system is initialized in $\hat{\rho}_0$, corresponding to the ground state at $\Omega(0)/\chi$, before the field is slowly ramped to $\Omega(\tau)$, described by unitary $\hat{U}(\tau)$. A global rotation is imprinted on the state before the dynamics are reversed via (i) a many-body echo $\hat{U}^\dagger(t)$ or (ii) a pseudoecho $\hat{U}_{\rm PE}(\tau)$. In the former, the sign of the Hamiltonian is also flipped; whereas in the latter, it is not. (b)–(c) Benchmark of dynamical protocol. The MQC components predicted from the exact ground state (faded blue lines) compared to those obtained from a pseudoecho ramping sequence of durations $\chi\tau = 10$ (black) and $\chi\tau = 100$ (red). All data are from numerical simulations using $N = 50$ and $N = 20$ for the LMG and TFI models, respectively (see Ref. [50] for details of ramps).

the Hamiltonian parameters in time. While we stress that our protocol is entirely generic, for simplicity, we focus here on the LMG and TFI models, which we later investigate numerically. Our sequence starts from the state $\hat{\rho}(0) = \hat{\rho}_{\rm GS}^P$ prepared at large $\Omega(0)/\chi \gg 1$ (for simplicity, we assume χ is fixed). The ratio of these parameters is slowly changed such that the instantaneous state of the system follows the ground state of the instantaneous Hamiltonian $\hat{H}(t)$ characterized by $\Omega(t)/\chi$, $\hat{\rho}(t) = \hat{U}(t)\hat{\rho}_0\hat{U}^\dagger(t) \equiv \hat{\rho}_{\rm GS}(t)$. A global rotation, $e^{-i\phi\hat{S}_x}$, is then imprinted on the state by, e.g., suddenly quenching to $\Omega(t)/\chi \gg 1$. Ideally, the echo is completed by flipping the sign of the instantaneous Hamiltonian such that $\hat{H}(t) \rightarrow -\hat{H}(2\tau - t)$ for $t > \tau$, where τ is the duration of the initial ramping sequence. However, the ability to control the sign of the Hamiltonian is out of reach in many state-of-the-art experiments.

To overcome this barrier and make our protocol more widely applicable, we propose that the MQC spectrum can still be exactly obtained using a *pseudoecho* [$\hat{U}_{\rm PE}(t)$ in Fig. 3(a)] where the sign of the Hamiltonian is *not* flipped, as long as the ramping sequence is sufficiently adiabatic. Finally, the overlap with $\hat{\rho}_{\rm GS}^P$ is obtained to yield F_ϕ. We justify the pseudoecho by the observation that the state produced by sequential adiabatic ramps of the transverse field from $\Omega(0) \rightarrow \Omega(t) \rightarrow \Omega(0)$ is effectively identical to that produced by true time reversal; i.e., the system will return to the initial ground state up to an overall irrelevant phase (see Ref. [50]).

This is a significant result as it demonstrates that effective time reversal can still be achieved in the absence of any control of the sign of the Hamiltonian. Moreover, we are able to extract detailed information about the coherences of the complex many-body state $\hat{\rho}(t)$ without technically challenging state tomography [64–67] or randomized measurements [68,69]. Instead, the coherent dynamics in the second half of the echo protocol map this information to a relatively manageable measurement (of the overlap with a simple product state [70]).

Numerical study of quasi-adiabatic ramps.—Realistically, technical constraints and decoherence preclude the possibility of truly adiabatic dynamics in an experiment. To address this issue, we investigate the robustness of the MQC spectrum to diabatic excitations generated in a realistic ramp of finite duration and demonstrate that it retains reliable signatures of the QPT [71].

In Figs. 3(b)–3(c), we present data for the previously discussed LMG and TFI models for ramps of duration $\chi\tau = (10, 100)$ starting in the paramagnetic phase. In both cases, we obtain the dynamics by numerically solving a time-dependent Schrödinger equation for small systems. For the LMG model, we take $N = 50$ and $\Omega(0) = 10$; while for the TFI model, $N = 20$ and $\Omega(0) = 10^2$, with both ramps tailored to reach $\Omega(\tau) = 10^{-2}$ [50]. We focus on the low-m individual intensities rather than the width $\sigma_{\rm MQC}$, because decoherence will typically make accessing large-m intensities, and thus the full spectrum, technically challenging. An important figure of merit is the fidelity with which the targeted ground state is prepared: $\mathcal{F} = |\langle\psi_{\rm GS}(\tau)|\psi(\tau)\rangle|^2$. For the ramp durations in Figs. 3(b)–3(c), the fidelities are $\mathcal{F} = (0.13, 0.99)$ and $\mathcal{F} = (0.5, 0.99)$ for the LMG and TFI models, respectively. Even for low fidelity ramps, the intensities obtained from the pseudoecho reasonably follow the predictions of the exact ground state [50], despite the generation of appreciable low-energy excitations. As a consequence, when interpreting connections between the MQC spectrum and the QPT, one should demonstrate that the physics observed is dominated by the $T = 0$ ground state. One way to quantify this is to measure a return fidelity after a pseudoecho in the absence of the perturbation, which is associated with $\mathcal{F}_{\phi=0}$ [50]. A large return fidelity approaching unity

indicates the MQC spectrum is dominated by the ground state contribution.

Experimental implementation.—Our proposal to diagnose equilibrium QPTs using quantum coherence can be implemented in a range of experimental platforms featuring sufficient control of quasi-adiabatic dynamics. Promising directions include trapped-ion quantum simulators of interacting spin models and quantum simulators of Hubbard-like models implemented with neutral atoms and Rydberg atoms in optical lattices aided by a quantum gas microscope [72] or in tweezer arrays [73,74]. Trapped ions [28,70,75–78] in particular can be used to simulate the TFI and LMG examples studied here in addition to more generic models with power-law spin-spin interactions mediated by phonons [50]. These systems feature sufficiently low decoherence rates to enable both the high-quality preparation of the entangled ground state [50,70,79] and the ability to measure state overlap [28]. While time reversal has been demonstrated in Penning traps in the limit of all-to-all interactions, which are mediated by coupling to a single phonon mode [28], the Hamiltonian sign cannot be controlled for more generic interactions mediated by multiple phonon modes, and thus the pseudoecho protocol we develop in this Letter is of immediate relevance.

Conclusion.—We have proposed and investigated a dynamical method to diagnose signatures of quantum coherence in a QPT using FOTOCs. Our approach is robust, has modest technical demands, and does not require time reversal through control of the sign of the Hamiltonian. While our numerical investigation focused on spin models implementable in arrays of trapped ions and Rydberg atoms, our results are broadly applicable to a range of AMO quantum simulators where ground state physics can be studied in a controlled and isolated environment.

We acknowledge helpful discussions with Cindy Regal, Mark Brown, and Itamar Kimchi. This work is supported by the AFOSR Grant No. FA9550-18-1-0319, the DARPA and ARO Grant No. W911NF-16-1-0576, the ARO Single Investigator Grant No. W911NF-19-1-0210, the NSF Grant No. PHY1820885, the NSF Grant No. JILA-PFC PHY-1734006, NSF Grant No. QLCI-2016244 and the NIST.

[1] S. Sachdev, *Quantum Phase Transitions*, 2nd ed. (Cambridge University Press, Cambridge, England, 2011).
[2] T. J. Osborne and M. A. Nielsen, Phys. Rev. A **66**, 032110 (2002).
[3] G. Vidal, J. I. Latorre, E. Rico, and A. Kitaev, Phys. Rev. Lett. **90**, 227902 (2003).
[4] J. Eisert, M. Cramer, and M. B. Plenio, Rev. Mod. Phys. **82**, 277 (2010).
[5] H. T. Quan, Z. Song, X. F. Liu, P. Zanardi, and C. P. Sun, Phys. Rev. Lett. **96**, 140604 (2006).
[6] P. Zanardi and N. Paunković, Phys. Rev. E **74**, 031123 (2006).
[7] S.-J. GU, Int. J. Mod. Phys. B **24**, 4371 (2010).
[8] A. F. Albuquerque, F. Alet, C. Sire, and S. Capponi, Phys. Rev. B **81**, 064418 (2010).
[9] L. Wang, Y.-H. Liu, J. Imriska, P. N. Ma, and M. Troyer, Phys. Rev. X **5**, 031007 (2015).
[10] J.-J. Chen, J. Cui, Y.-R. Zhang, and H. Fan, Phys. Rev. A **94**, 022112 (2016).
[11] G. Karpat, B. Çakmak, and F. F. Fanchini, Phys. Rev. B **90**, 104431 (2014).
[12] Y.-C. Li and H.-Q. Lin, Sci. Rep. **6**, 26365 (2016).
[13] Y. C. Li, J. Zhang, and H.-Q. Lin, Phys. Rev. B **101**, 115142 (2020).
[14] M.-L. Hu, Y.-Y. Gao, and H. Fan, Phys. Rev. A **101**, 032305 (2020).
[15] R. J. Lewis-Swan, A. Safavi-Naini, A. M. Kaufman, and A. M. Rey, Nat. Rev. Phys. **1**, 627 (2019).
[16] A. Polkovnikov, K. Sengupta, A. Silva, and M. Vengalattore, Rev. Mod. Phys. **83**, 863 (2011).
[17] P. Hayden and J. Preskill, J. High Energy Phys. 09 (2007) 120.
[18] Y. Sekino and L. Susskind, J. High Energy Phys. 10 (2008) 065.
[19] S. H. Shenker and D. Stanford, J. High Energy Phys. 03 (2014) 067.
[20] A. Kitaev, in *Proceedings of the Fundamental Physics Prize Symposium, 2014* (unpublished).
[21] M. Heyl, F. Pollmann, and B. Dóra, Phys. Rev. Lett. **121**, 016801 (2018).
[22] B. Chen, X. Hou, F. Zhou, P. Qian, H. Shen, and N. Xu, Appl. Phys. Lett. **116**, 194002 (2020).
[23] H. Shen, P. Zhang, R. Fan, and H. Zhai, Phys. Rev. B **96**, 054503 (2017).
[24] C. B. Dağ, K. Sun, and L.-M. Duan, Phys. Rev. Lett. **123**, 140602 (2019).
[25] X. Nie, B.-B. Wei, X. Chen, Z. Zhang, X. Zhao, C. Qiu, Y. Tian, Y. Ji, T. Xin, D. Lu, and J. Li, Phys. Rev. Lett. **124**, 250601 (2020).
[26] R. J. Lewis-Swan, A. Safavi-Naini, J. J. Bollinger, and A. M. Rey, Nat. Commun. **10**, 1581 (2019).
[27] M. Gärttner, P. Hauke, and A. M. Rey, Phys. Rev. Lett. **120**, 040402 (2018).
[28] M. Gärttner, J. G. Bohnet, M. Safavi-Naini, M. L. Wall, J. J. Bollinger, and A. M. Rey, Nat. Phys. **13**, 781 (2017).
[29] J. Baum, M. Munowitz, A. N. Garroway, and A. Pines, J. Chem. Phys. **83**, 2015 (1985).
[30] M. Munowitz, A. Pines, and M. Mehring, J. Chem. Phys. **86**, 3172 (1987).
[31] P. Cappellaro, in *Quantum State Transfer and Network Engineering* (Springer, New York, 2014), pp. 183–222.
[32] J. Li, R. Fan, H. Wang, B. Ye, B. Zeng, H. Zhai, X. Peng, and J. Du, Phys. Rev. X **7**, 031011 (2017).
[33] E. J. Meier, J. Ang'ong'a, F. A. An, and B. Gadway, Phys. Rev. A **100**, 013623 (2019).
[34] K. X. Wei, C. Ramanathan, and P. Cappellaro, Phys. Rev. Lett. **120**, 070501 (2018).
[35] G. Zhu, M. Hafezi, and T. Grover, Phys. Rev. A **94**, 062329 (2016).
[36] B. Swingle, G. Bentsen, M. Schleier-Smith, and P. Hayden, Phys. Rev. A **94**, 040302(R) (2016).

[37] N. Y. Yao, F. Grusdt, B. Swingle, M. D. Lukin, D. M. Stamper-Kurn, J. E. Moore, and E. A. Demler, arXiv:1607.01801.

[38] K. A. Landsman, C. Figgatt, T. Schuster, N. M. Linke, B. Yoshida, N. Y. Yao, and C. Monroe, Nature (London) **567**, 61 (2019).

[39] P. D. Blocher, S. Asaad, V. Mourik, M. A. I. Johnson, A. Morello, and K. Mlmer, arXiv:2003.03980.

[40] B. Vermersch, A. Elben, L. M. Sieberer, N. Y. Yao, and P. Zoller, Phys. Rev. X **9**, 021061 (2019).

[41] M. K. Joshi, A. Elben, B. Vermersch, T. Brydges, C. Maier, P. Zoller, R. Blatt, and C. F. Roos, Phys. Rev. Lett. **124**, 240505 (2020).

[42] K. Macieszczak, E. Levi, T. Macrì, I. Lesanovsky, and J. P. Garrahan, Phys. Rev. A **99**, 052354 (2019).

[43] S. L. Braunstein and C. M. Caves, Phys. Rev. Lett. **72**, 3439 (1994).

[44] P. Hauke, M. Heyl, L. Tagliacozzo, and P. Zoller, Nat. Phys. **12**, 778 (2016).

[45] H. Lipkin, N. Meshkov, and A. Glick, Nucl. Phys. **62**, 188 (1965).

[46] P. Ribeiro, J. Vidal, and R. Mosseri, Phys. Rev. Lett. **99**, 050402 (2007).

[47] P. de Gennes, Solid State Commun. **1**, 132 (1963).

[48] R. B. Stinchcombe, J. Phys. C **6**, 2459 (1973).

[49] A. Dutta, G. Aeppli, B. K. Chakrabarti, U. Divakaran, T. F. Rosenbaum, and D. Sen, *Quantum Phase Transitions in Transverse Field Spin Models: From Statistical Physics to Quantum Information* (Cambridge University Press, Cambridge, England, 2015).

[50] See Supplemental Material at http://link.aps.org/supplemental/10.1103/PhysRevLett.125.240605, for details of quasi-adiabatic ramps, analytical treatments of LMG and TFI models, discussions of finite-size effects and decoherence, and extensions to nonintegrable models, which includes Refs. [51–61].

[51] P. Richerme, C. Senko, S. Korenblit, J. Smith, A. Lee, R. Islam, W. C. Campbell, and C. Monroe, Phys. Rev. Lett. **111**, 100506 (2013).

[52] S. Balasubramanian, S. Han, B. T. Yoshimura, and J. K. Freericks, Phys. Rev. A **97**, 022313 (2018).

[53] P. Pfeuty, Ann. Phys. (Berlin) **57**, 79 (1970).

[54] I. S. Gradshteyn and I. M. Ryzhik, *Table of Integrals, Series, and Products*, 7th ed. (Academic Press, San Diego, CA, 2007).

[55] H.-M. Kwok, W.-Q. Ning, S.-J. Gu, and H.-Q. Lin, Phys. Rev. E **78**, 032103 (2008).

[56] D. F. Walls and G. J. Milburn, *Quantum Optics*, 2nd ed. (Springer-Verlag, Berlin, 2008).

[57] W. Ge, B. C. Sawyer, J. W. Britton, K. Jacobs, J. J. Bollinger, and M. Foss-Feig, Phys. Rev. Lett. **122**, 030501 (2019).

[58] K. Kim, M.-S. Chang, R. Islam, S. Korenblit, L.-M. Duan, and C. Monroe, Phys. Rev. Lett. **103**, 120502 (2009).

[59] P. Jurcevic, B. P. Lanyon, P. Hauke, C. Hempel, P. Zoller, R. Blatt, and C. F. Roos, Nature (London) **511**, 202 (2014).

[60] B. K. Chakrabarti, A. Dutta, and P. Sen, *Quantum Ising Phases and Transitions in Transverse Ising Models* (Springer-Verlag, Berlin, 1996).

[61] C. Karrasch and D. Schuricht, Phys. Rev. B **87**, 195104 (2013).

[62] B. Damski, Phys. Rev. E **87**, 052131 (2013).

[63] L. Cincio, M. M. Rams, J. Dziarmaga, and W. H. Zurek, Phys. Rev. B **100**, 081108(R) (2019).

[64] H. Häffner, W. Hänsel, C. F. Roos, J. Benhelm, D. Chek-al kar, M. Chwalla, T. Körber, U. D. Rapol, M. Riebe, P. O. Schmidt, C. Becher, O. Gühne, W. Dür, and R. Blatt, Nature (London) **438**, 643 (2005).

[65] D. Gross, Y.-K. Liu, S. T. Flammia, S. Becker, and J. Eisert, Phys. Rev. Lett. **105**, 150401 (2010).

[66] B. P. Lanyon, C. Maier, M. Holzäpfel, T. Baumgratz, C. Hempel, P. Jurcevic, I. Dhand, A. S. Buyskikh, A. J. Daley, M. Cramer, M. B. Plenio, R. Blatt, and C. F. Roos, Nat. Phys. **13**, 1158 (2017).

[67] G. Torlai, G. Mazzola, J. Carrasquilla, M. Troyer, R. Melko, and G. Carleo, Nat. Phys. **14**, 447 (2018).

[68] A. Elben, B. Vermersch, C. F. Roos, and P. Zoller, Phys. Rev. A **99**, 052323 (2019).

[69] T. Brydges, A. Elben, P. Jurcevic, B. Vermersch, C. Maier, B. P. Lanyon, P. Zoller, R. Blatt, and C. F. Roos, Science **364**, 260 (2019).

[70] A. Safavi-Naini, R. J. Lewis-Swan, J. G. Bohnet, M. Gärttner, K. A. Gilmore, J. E. Jordan, J. Cohn, J. K. Freericks, A. M. Rey, and J. J. Bollinger, Phys. Rev. Lett. **121**, 040503 (2018).

[71] As our consideration of nonadiabatic ramps is specifically motivated by limitations on ramp duration due to decoherence, we do not directly consider the effects of decoherence on the MQC spectrum in detail. A brief discussion of the expected relevance of decoherence may instead be found in Ref. [50].

[72] C. Gross and I. Bloch, Science **357**, 995 (2017).

[73] A. Keesling, A. Omran, H. Levine, H. Bernien, H. Pichler, S. Choi, R. Samajdar, S. Schwartz, P. Silvi, S. Sachdev, P. Zoller, M. Endres, M. Greiner, V. Vuletic, and M. D. Lukin, Nature (London) **568**, 207 (2019).

[74] A. Browaeys and T. Lahaye, Nat. Phys. **16**, 132 (2020).

[75] P. Richerme, C. Senko, J. Smith, A. Lee, S. Korenblit, and C. Monroe, Phys. Rev. A **88**, 012334 (2013).

[76] P. Jurcevic, H. Shen, P. Hauke, C. Maier, T. Brydges, C. Hempel, B. P. Lanyon, M. Heyl, R. Blatt, and C. F. Roos, Phys. Rev. Lett. **119**, 080501 (2017).

[77] J. Zhang, G. Pagano, P. Hess, A. Kyprianidis, P. Becker, H. Kaplan, A. Gorshkov, Z.-X. Gong, and C. Monroe, Nature (London) **551**, 601 (2017).

[78] M. L. Wall, A. Safavi-Naini, and A. M. Rey, Phys. Rev. A **95**, 013602 (2017).

[79] A. Safavi-Naini, R. J. Lewis-Swan, J. G. Bohnet, M. Garttner, K. A. Gilmore, E. Jordan, J. Cohn, J. K. Freericks, A. M. Rey, and J. J. Bollinger, arXiv:1711.07392.